

Seismic Dynamic Damage Analysis of High-Rise Water Intake Tower

Jing Ma¹, ShiJie Xu¹, Xiaodong Zheng^{1,2*}, YunBao Zhang²

¹ Hebei University of Engineering, Handan, Hebei, China

² Hebei Institute of Water Science, Shijiazhuang, Hebei, China

*Corresponding Author.

Abstract:

Intake tower is as important as other buildings in water conservancy and hydropower projects. It involves the normal operation of the entire water diversion and discharge system. Therefore, the anti-seismic safety of intake tower is very important to the safety of water control project. This study simulates the seismic response of an intake tower, both with and without concrete damage. We employ the constitutive model for elastoplastic concrete damage and combine it with actual water intake tower engineering data to establish a three-dimensional finite element model for the water intake tower body and foundations using ABAQUS software. The results show that the stress and strain of the intake tower are higher when concrete damage is considered. Tensile and compressive damage of the tower body predominantly occurs at the junction between the tower body and the backfilled concrete. As the earthquake duration increases, the degree and extent of water intake tower damage gradually increase. Therefore, the safety of the intake tower is reduced, but it is more in line with the actual project. These research results provide important scientific insights for high-rise intake tower project planning in areas prone to strong earthquakes.

Keywords: High-rise water intake tower, Strong earthquake, Stress-strain analysis, Damage mechanism.

I. INTRODUCTION

Water intake towers are an important hydraulic structure independent of the dam and at the forefront of the diversion and drainage system. The design of an intake tower is not only related to its own function but also considers the normal operation of the entire diversion and drainage system. Moreover, seismic resistance of intake towers is crucial for ensuring the safety of water conservation [1]. At present, China is in an important period of hydropower development. For example, the Linsang Xiao Wan project in Yunnan, the Xiluodu project on the Jinsha River, the Jinping project on the Yalong River, and the Laxiwa Hydropower Station on the upper reaches of the Yellow River have dam heights of 292 m, 276 m, 305 m, and 250 m, respectively, with corresponding intake tower heights of more than 100 m [2]. Therefore, the safety of the entire diversion and drainage system and even the dam itself is an important area of research.

Seismic research of high-rise tower structures has made some important advances. Chen [3] suggested a calculation model for an intake tower structure that treats the intake tower as a plane frame structure to determine the relevant internal forces and stresses. However, the model is very simplified, which results in

large calculation errors. Zheng [4] compared the differences in elastic connection and dynamic contact methods for intake towers and discussed the dynamic characteristics and response laws of the intake tower interaction system. Li [5] employed a time-history analysis method and response spectrum analysis method to determine the seismic load curve, revealing the importance of using dynamic contact to analyze the combined dynamic interactions between the intake tower and the rock mass. However, many previous studies on intake towers are based on the linear elastic material of the tower body [6-7], and few have considered in the damage to a concrete high-rise intake tower under strong earthquake motion. Therefore, this study establishes an elastoplastic damage model for concrete. This constitutive model is combined with data from an actual intake tower project to develop a more realistic three-dimensional finite element model for the tower body plus foundations. The seismic response of the intake tower is determined both with and without concrete damage. The results provide crucial data for the seismic resistance and safety of water intake tower structures.

II. ELASTOPLASTIC DAMAGE CONSTITUTIVE MODEL

Under the action of seismic load, cracking of a concrete dam is mainly a result of tension, whereas crushing of the dam due to pressure is rare [8]. This is because the tensile strength of concrete is much smaller than its compressive strength, and the safety factor of compressive strength in the dam body design is relatively large; therefore, many scholars have focused on the evolution of concrete tensile damage [9-11]. The model of Lee et al. is improved by combining damage mechanics and plastic mechanics to establish a plastic damage model that considered the irreversible residual variables caused by damage [12]. In order to allow more realistic and convenient descriptions of structural damage when deriving the constitutive damage model, the initial elastic strain, the damaging strain with residual variables, and the inelastic strain are introduced into the free energy function. That is, the free energy, ψ , can be expressed as

$$\psi = \psi(\varepsilon^{el}, \varepsilon^{enl}, \varepsilon^p, \theta, V_k) \quad (1)$$

Where ε^{el} represents the elastic strain tensor; ε^p represents the unrecoverable residual strain tensor; ε^{enl} represents the inelastic strain tensor caused by the decrease in stiffness; θ represents the temperature; V_k represents the internal variable.

Regarding the unrecoverable residual deformation, the free energy can be divided into the non-elastic part, elastic part, and unrecoverable residual part. In the case of an isothermal adiabatic process, the damage variable, D , is used to represent the internal variable V_k . Thus, eq. (1) can be rewritten as

$$\psi(\varepsilon^{el}, \varepsilon^{enl}, \varepsilon^p, D) = \psi^{el}(\varepsilon^{el}, D) + \psi^{enl}(\varepsilon^{enl}, D) + \psi^p(\varepsilon^p, D) \quad (2)$$

Where $\psi^{el}(\varepsilon^{el}, D)$ represents the elastic free energy; $\psi^p(\varepsilon^p, D)$ represents the irreversible residual strain free energy, $\psi^{enl}(\varepsilon^{enl}, D)$ represents the inelastic strain free energy.

As concrete material is assumed to be isotropic, a single scalar quantity, D , is used to represent the damage variable, which is the elastic free energy of the concrete material $\psi^{el}(\varepsilon^{el}, D)$. D can be expressed as

$$\psi^{el}(\varepsilon^{el}, D) = \frac{1}{2\rho}(1-D)\varepsilon^{el} : C_0 : \varepsilon^{el} = \frac{1}{2\rho}(1-D)\sigma : \varepsilon^{el} = (1-D)\psi_0^{el}(\varepsilon^{el}) \quad (3)$$

Where C_0 represents the initial stiffness tensor of the concrete;

The concrete damage constitutive relationship can be expressed as

$$\sigma = \rho \frac{\partial \psi^{el}(\varepsilon^{el}, D)}{\partial \varepsilon^{el}} \quad (4)$$

For known materials, the total free energy is determined, which is the plastic-free energy, using the following expression.

$$\begin{aligned} \psi^d(\varepsilon^d, D) &= \psi^e(\varepsilon^e, D) + \psi^p(\varepsilon^p, D) \\ &= \varphi(\varepsilon^{el}, \varepsilon^{enl}) + \phi(\varepsilon^{el}, \varepsilon^p) \end{aligned} \quad (5)$$

Where $\varphi(\varepsilon^{el}, \varepsilon^{enl})$ and $\phi(\varepsilon^{el}, \varepsilon^p)$ represent functions containing the strain and internal strain. We then assume that the damage energy release rate, Y , is the adjoint variable of the damage variable D ; i.e., the damage energy release rate expression is

$$Y = -\rho[1 + \varphi(\varepsilon^{el}, \varepsilon^{enl})] + \phi(\varepsilon^{el}, \varepsilon^p) \frac{\partial \psi^{el}(\varepsilon^{el}, D)}{\partial D} \quad (6)$$

The damage evolution expression can then be written as

$$D_{C,I} = 1 - \exp\left(-\frac{(Y_{C,I} - Y_{C,0I})^{a_{C,I}}}{b_{C,I}}\right) \quad (7)$$

Where $Y_{C,0I}$ represents the initial damage threshold under pressure and tension; $D_{C,I}$ represents the damage variable under pressure and tension; $a_{C,I}$ and $b_{C,I}$ represent material parameters.

In this study, the yield criterion of the Lee-Fenves model in the effective space is selected, and the hardening parameter is determined as the equivalent plastic strain [13]. The yield criterion can be expressed as

$$F(\sigma, \mathcal{I}^p) = \frac{1}{1-\alpha} \left[\alpha \mathcal{I}_1^p + \sqrt{3\mathcal{I}_2^p} + \beta(\mathcal{I}^p) \langle \hat{\sigma}_{\max} \rangle \right] - c(\mathcal{I}_c^p) \quad (8)$$

$$\alpha = \frac{(f_{b0} / f_{c0}) - 1}{2(f_{b0} / f_{c0}) - 1} \quad (9)$$

$$\beta = \frac{\bar{c}_c(\mathcal{I}_c^p)}{\bar{c}_t(\mathcal{I}_c^p)} (1 - \alpha) - (1 + \alpha) \quad (10)$$

$$c = \bar{c}_c(\mathcal{I}_c^p) \quad (11)$$

Where c is effective cohesion; $\hat{\sigma}_{\max}$ is maximum effective principal stress; f_{b0} / f_{c0} is ratio of biaxial isobaric to uniaxial compression strength, usually 1.16; $\bar{c}_t(\mathcal{I}_c^p)$ is uniaxial tension effective stress; $\bar{c}_c(\mathcal{I}_c^p)$ is uniaxial compression effective stress; \mathcal{I}_2^p is the second invariant; \mathcal{I}_1^p is the first invariant;

In order to derive the plastic flow size and direction, the plastic flow rule needs to be defined. For concrete, the non-associative flow rule is used [14]. The plastic potential function G can be written as

$$G = \sqrt{2\mathcal{I}_2^p} + \alpha^p \mathcal{I}_1^p \quad (12)$$

Where α^p is the expansion angle.

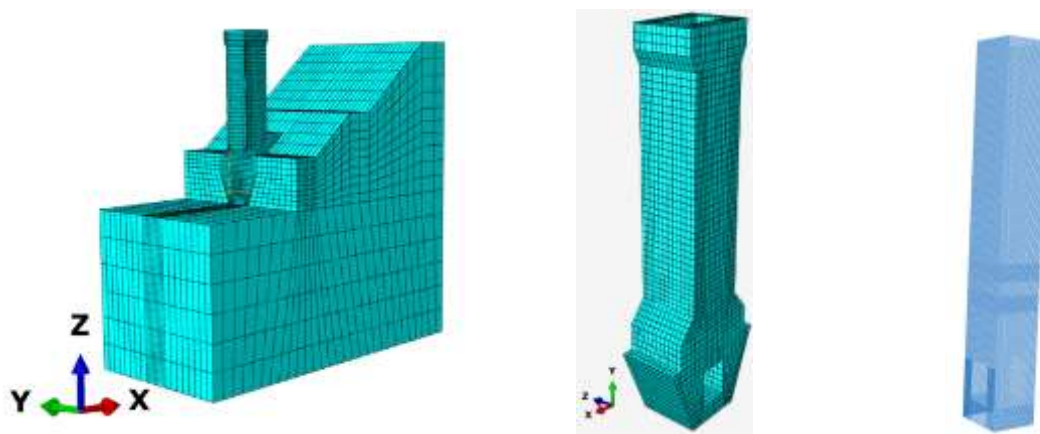
The compression (tension) damage variables are introduced into the elastic free energy and the plastic free energy respectively, the compressive (tensile) damage constitutive equation of concrete can be obtained.

$$\begin{cases} \sigma_t = (1 - D_t) E_0 (\varepsilon_t - \varepsilon_t^{enl} - \varepsilon_t^p) \\ \sigma_c = (1 - D_c) E_0 (\varepsilon_c - \varepsilon_c^{enl} - \varepsilon_c^p) \end{cases} \quad (13)$$

Where σ_t represents concrete tensile damage constitutive equation; ε_t represents the tensile strain; ε_t^{enl} represents the tensile inelastic strain; ε_t^p represents tensile residual strain; D_t represents the tension damage variable; σ_c represents concrete compression damage constitutive equation; ε_c represents the compression strain; ε_c^{enl} represents the compression inelastic strain; ε_c^p represents compression residual strain; D_c represents the compression damage variable; E_0 represents the elastic modulus without material damage.

III. MODEL OVERVIEW

Modeling is conducted for a water intake tower of a hydropower station, where the maximum height of the water intake tower is 2721 m, the bottom plate height of the water intake is 2640 m, the bottom plate thickness is 5 m, the foundation depth and length on the upper and lower sides is equal to the height of the tower body, the length of the foundation on the left and right sides is 40 m, and the height of the rock mass at the back of the tower is 80 m. The steel bars in the intake tower are embedded in the concrete, and there is no sliding between the steel bars and the concrete. The model of the intake tower body and foundation is shown in Fig. 1.



(a) The intake tower and foundation system (b) The tower body (c) Reinforcement Element

Fig. 1. Intake tower finite element model

A finite element model of the intake tower body and foundation is established using ABAQUS finite element software. A C3D8R solid unit is adopted for both the intake tower and foundation adopting a Cartesian calculation coordinate system. The coordinate origin is selected as the center point of the front edge above the bottom plate of the intake tower. The positive direction of the X-axis is the direction of downstream water flow, the positive direction of the Y-axis is perpendicular to the direction of water flow, and the positive direction of the Z-axis is perpendicular to the top of the tower.

The "Specification for Load Design of Hydraulic Structures"[15] and "Design Code for Hydraulic Concrete Structures"[16] are used as reference material, and the selected concrete mechanical parameters are shown in Table I. The concrete strength grades for the flood discharge tunnel intake tower (< 2663 m elevation), the tower drum (> 2663 m elevation), and the backfill concrete of the tower back (2660–2680 m elevation) are C₃₀, C₂₅, and C₂₀, respectively. The influence of steel reinforcement is not considered in the model.

TABLE I. Concrete mechanical parameters

Concrete power level	Static axial compressive strength (MPa)	Dynamic axial compressive strength (MPa)	Dynamic axial tensile strength (MPa)	Static modulus of elasticity (MPa)	Poisson's ratio
C20	18.5	24.1	2.41	2.55×10^4	0.167
C25	22.4	29.1	2.91	2.80×10^4	0.167
C30	26.2	34.1	3.41	3.00×10^4	0.167

According to the elastoplastic damage model calculation formula in equation (5), the elastoplastic constitutive relationship for different concrete grades and the damage evolution relationship of concrete are obtained. The foundation is analyzed using linear elasticity. The concrete partition map of the intake tower is shown in Fig. 2.

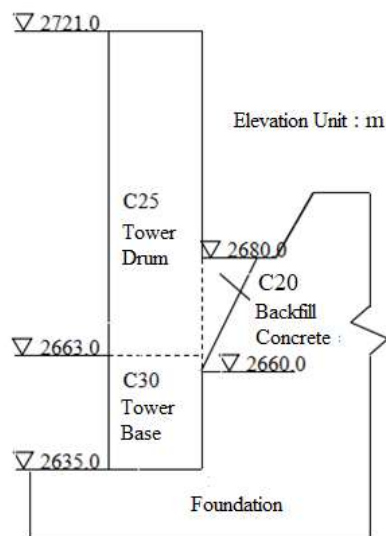
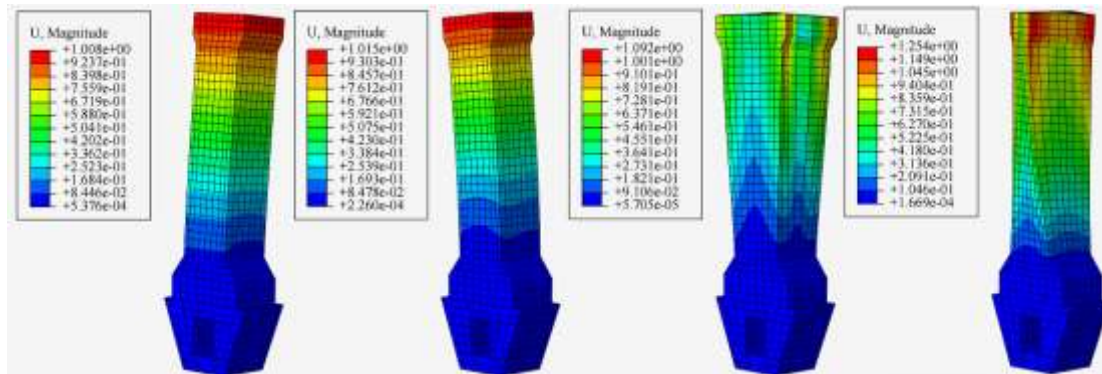


Fig. 2. Intake tower concrete partition map

The first step of seismic dynamic analysis is to solve the dynamic characteristics of the structure. The natural vibration period and frequency of each order of the structure can be obtained by modal analysis. The modal analysis shows that the natural vibration frequency of the first four orders of the water intake tower is 2.097Hz, 2.264Hz, 5.313Hz, 7.975Hz. The first four order vibration modes of the intake tower are shown in Fig. 3.

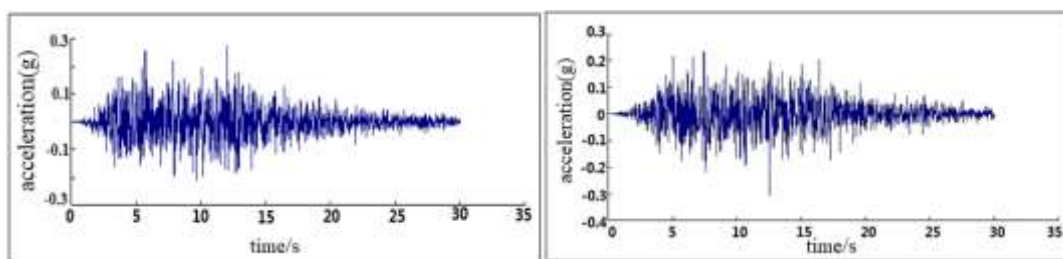


(a)The first order (b) The second order (c) The third order (d) The four order

Fig.3 Intake tower four vibration modes

The hydrodynamic pressure is simulated using the Westergaard additional mass method [17]. The Rayleigh damping coefficient is calculated according to the frequency of the dam-foundation system; $\alpha = 0.8539 \text{ s}^{-1}$ and $\beta = 0.0028$ where the damping ratio, $\xi = 0.05$, and foundation radiation damping are analyzed using artificial viscoelastic boundaries [18].

According to the project reference data and the Code for Seismic Design of Hydraulic Structures (SL203-97), the intake tower is a Class 1 hydraulic structure. The seismic fortification category of the project is Class A, and the engineering site category is Class I earthquake fortification. The intensity is 8° and the basic intensity is 7° . In this study, ground motion parameters with a probability of 2% in the base period are selected for the model earthquake [3]. The corresponding horizontal ground motion peak acceleration is 0.304 g, the characteristic period, T_g is 0.2 s, and the design response spectrum maximum, β_{\max} is 6.71. According to the provisions of the Code for Seismic Design of Buildings (GB50011-2010), the peak ratio of seismic waves input in three directions is X: Y: Z=1:0.85:0.65. Three artificial seismic waves are fitted, whose total duration is 30 s and the time step is 0.01 s, as shown in Fig. 4.



(a) X direction

(b) Y direction

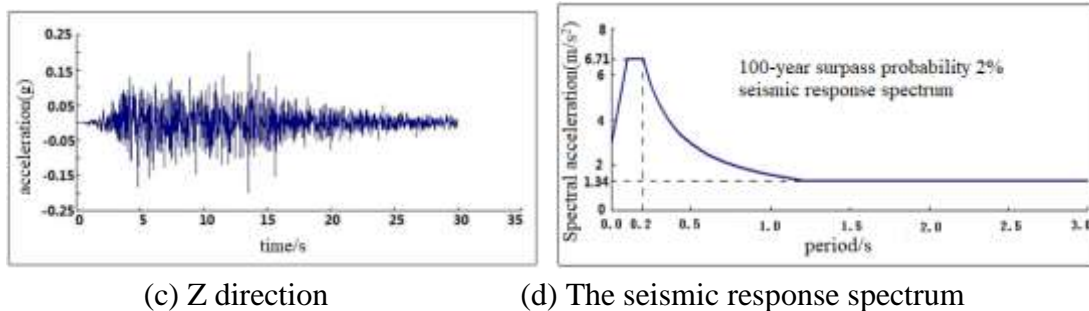


Fig. 4. Design of the artificial seismic wave used in this study

IV. STRESS-STRAIN ANALYSIS OF INTAKE TOWER

Because the structure is easy to produce the stress concentration at the sudden change of geometry and material property, and it is easy to produce the maximum displacement at the top of the intake tower [9], we select three key points of the intake tower, as shown in Fig. 5. The three directions of ground motion; i.e., the X-direction seismic wave along with the water flow, the Y-direction seismic wave, and the vertical Z-direction seismic wave in the vertical flow, are simultaneously input. The artificial ground motion design is shown in Fig. 4. The comparison analysis considers both damage and no damage and determines the differences in displacement for key points in the tower, the differences between stress and strain, and the changes in stress and strain within the tower body.

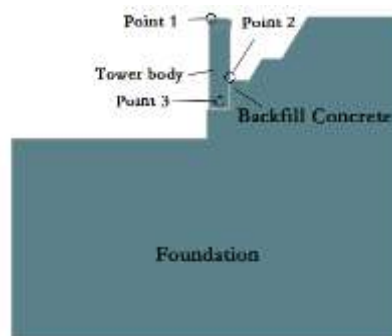


Fig. 5. Schematic diagram of the key points of the intake tower body

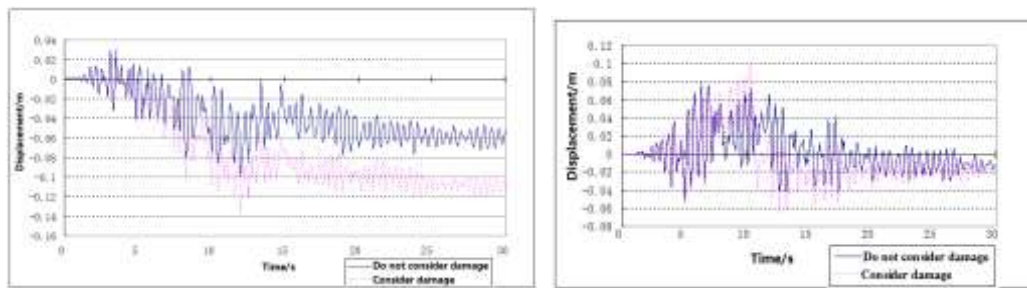
4.1 Comparison of Tower Displacement

According to the dynamic simulation analysis of the intake tower, the displacement is greatest at the top of the intake tower under strong earthquake motion. Table II shows the maximum displacement table of key point 1, both with and without concrete damage to the intake tower. Fig.6. shows displacement time history curve of key point 1.

TABLE II. The maximum displacement of key point 1 at the top of the tower

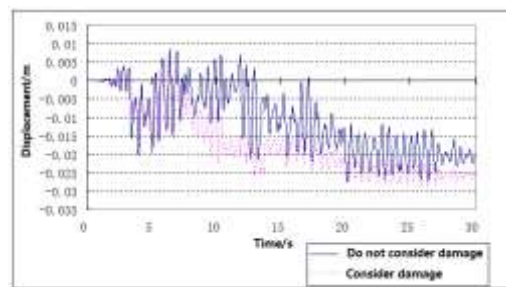
Displacement direction component	Calculation situation	Positive displacement (cm)	Growth rate	Occasion moment (s)	Negative displacement (cm)	Growth rate	Occasion moment (s)
Along the water X direction	Without damage	3.05	-3.1%	3.6	9.96	36.2%	12.2
	With damage	2.96		3.82	13.57		12.16
Vertical flow Y direction	Without damage	7.97	23.6%	6.48	5.29	18.3%	12.52
	With damage	9.85		10.48	6.26		12.84
Vertical Z direction	Without damage	0.52	9.71%	5.92	2.76	3.2%	26.80
	With damage	0.57		6.48	2.85		26.76

Note: Growth rate = (displacement with damage - displacement without damage) / displacement without damage



(a) X Direction Displacement

(b) Y Direction Displacement



(c) Z Direction Displacement

Fig.6. Displacement time history curve of key point 1 at Tower top

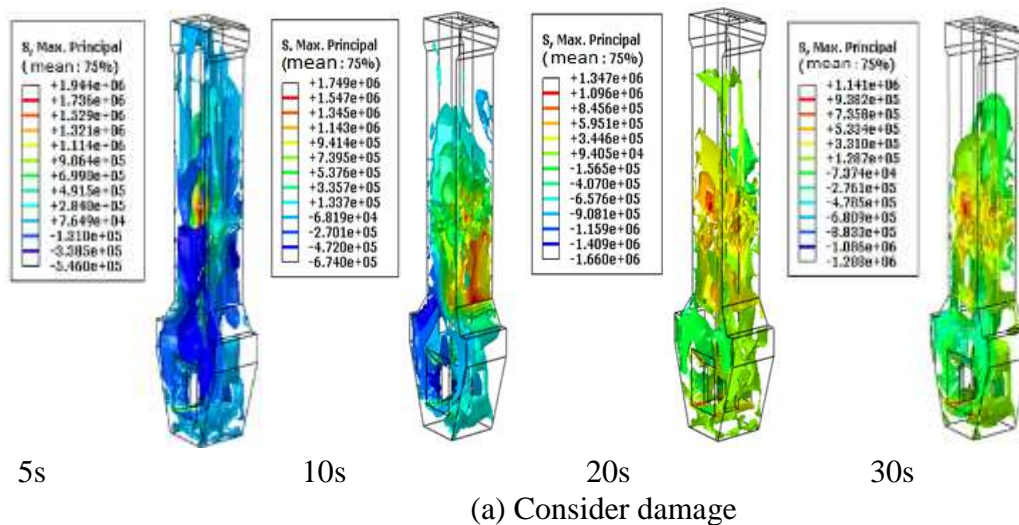
According to Tab.2 and Fig.6, the displacements in all directions typically increase when damage to the tower body concrete is considered. Only the X positive displacement exhibits a slight decrease, whereas the X negative displacement increases by the greatest amount, which is much greater than the displacement changes in the other two directions. This is predominant because X has a rock body at the back of the tower and the backfill concrete constrains the tower in the X positive direction; therefore, the energy of the concrete moving in the X direction is forced to converge in the negative X direction. The

resulting concrete damage is more serious, so the displacement change is greater. Then, due to the reduction in the corresponding X positive movement energy, the tower top displacement is reduced slightly. The positive and negative directions of the Y direction are symmetrical and unconstrained, so the displacement at the top of the tower increases significantly when considering concrete damage, with a similar magnitude in the positive and negative directions. The Z-direction is the vertical direction. Because of the strong interaction between the foundations and gravity, the maximum displacement in the positive and negative directions does not exhibit significant changes. Moreover, with concrete damage, the maximum displacement at the tower top does not change substantially. Therefore, displacement of the tower body increases but, due to the complexity of the structural form, the displacement changes differ in different directions. As such, the non-linear analysis results that do not consider concrete damage are unreliable.

It can be concluded that there is no change at the moment when the maximum displacement of the tower top is considered after the concrete is damaged. This also indicates that it is not the concrete damage that determines the dynamic response of the tower body, but the structure of the tower itself and the received load.

4.2 Comparison of Intake Tower Stress

Concrete is quasi-brittle, so the principal stress is typically used as the evaluation indicator. Fig.7.shows the Maximum principal stress nephogram of the tower under consideration of two cases without considering the damage of concrete. Under the two conditions, the stress distribution time-history of the intake tower body is basically the same, the large stress area of the tower body is both the tower base and the tower waist, and the stress concentration area is the junction area of the tower back and backfill. However, the maximum principal stress is slightly smaller when considering damage.



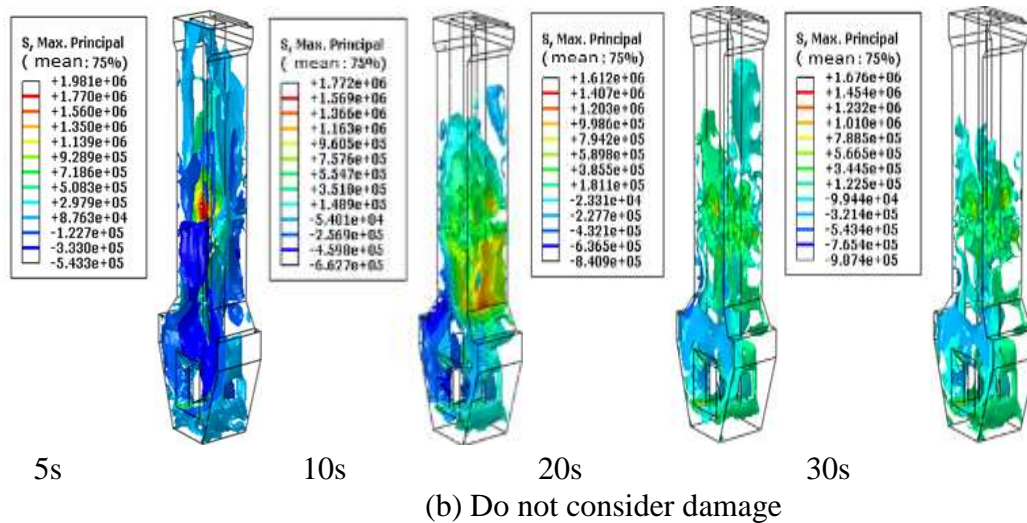
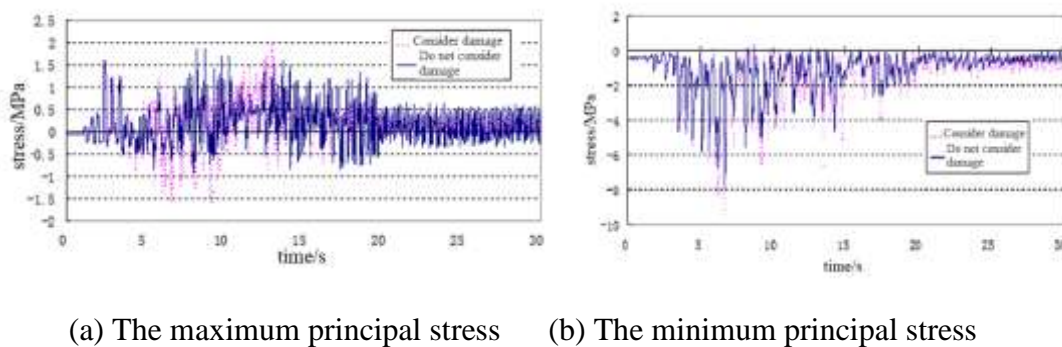


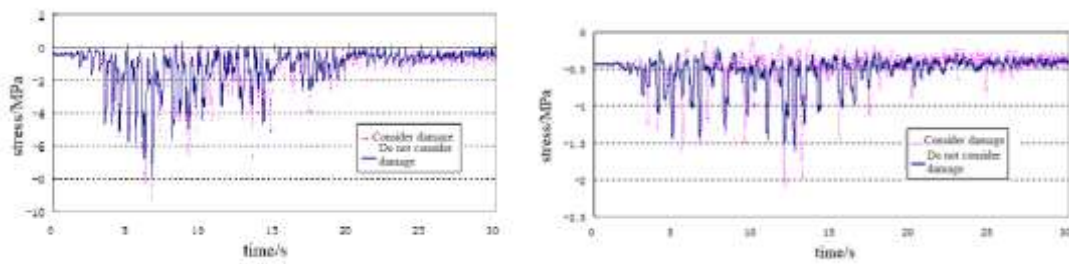
Fig.7. The Maximum principal stress nephogram of the tower

Fig. 8 and Fig. 9 show the principal stress-time history curve of key point 2 in the tower stress concentration area and key point 3 in the upper part of the tower, respectively. Key point 2 is in the initial stage of the earthquake (Fig. 8). Because the earthquake is not strong, the concrete in the tower body has not been damaged, and the material properties have not changed. Therefore, the main stress of the tower body is approximately the same in both cases. With earthquake magnitude increases, concrete damage accumulates, resulting in degradation of the mechanical properties of the material at key point 2. As the compressive strength of concrete is much greater than the tensile strength, the tensile strength degenerates, causing that the tensile stress at this stage is smaller than that without considering concrete damage, further resulting in energy transfer to the pressure stage. The compressive strength is so great that there is almost no degradation; thus, the compressive stress at this stage is greater than that without considering concrete damage. At the end of earthquake motion, the seismic load tends to be stable, so the principal stress of key point 2 tends to be small, and the principal stress in both cases is stable at the stress level of the static phase.



(a) The maximum principal stress (b) The minimum principal stress

Fig. 8. Principal stress-time history curve of key point 2 in the tower



(a) The maximum principal stress

(b) The minimum principal stress

Fig. 9. Principal stress-time history curve of key point 3 in the tower

According to Fig.9, the stress changes at key point 3 are approximately the same in the situation of both with and without concrete damage and increase after 5 s of earthquake motion. Due to the occurrence and accumulation of concrete damage, the stiffness is reduced and the stress level increased. At later stages of the earthquake, the stress level gradually decreases and remains approximately stable and the damage also becomes more stable; the level of stability remains approximately the same in both cases.

In summary, key point 2 is the stress concentration point at the back of the tower, and key point 3 is a general point in the upper part of the tower. The stress history curves of these two points indicate that considering concrete damage in the model, the stress amplitude increases, but the frequency spectrum of stress time history is basically the same.

4.3 Comparison of Intake Tower Strain

The intake tower shakes back and forth under earthquake motion to generate moments. Due to the tower's own gravity, the tensile and compressive strain is greatest in the vertical direction. Therefore, the influence of tower strain is analyzed by studying the changes in the elastic strain and non-elastic strain of the tower, considering the damage to the concrete and failure of the concrete.

According to Figs. 10(a) and 11(a), when concrete damage is considered, the amplitude of elastic strain changes in the concrete increases during earthquake motion. Specifically, strain increases greatly at key point 2, but the variation range does not change substantially. This is mainly because of that when the tower body is considered to be damaged, the stiffness of the tower body concrete gradually decreases during the earthquake and the strain naturally increases under the same stress level. Key point 2 is the stress concentration area. The degree of damage is severe and the stiffness is significantly reduced; thus, the increase in strain amplitude is large. Key point 3 is the general stress area, which has a low-stress level, and the light degree of damage; thus, the rigidity is not reduced significantly and the increase in strain amplitude is small. Because small-scale damage does not affect the basic structural performance of the tower structure, the range of strain changes at key points 2 and 3 does not change substantially.

Figs. 10(b) and 11(b) illustrate the inelastic strain history curves of key points 2 and 3, which are irrecoverable residual strains that increase as a function of time. The inelastic strain at key point 2 is zero from approximately 0–4 s; it then increases gradually after 4 s and tends to be stable after 20 s (Fig. 10(b)). Considering the inelastic strain increase at key point 2 after concrete damage, this is due to a reduction in the stiffness of the concrete due to seismic motion. Under the same earthquake action, key point 2 enters a high strain level, so an additional non-recoverable residual strain is added. The inelastic strain of point 3 is zero from approximately 0–7 s; it then suddenly increases after 7 s then remains approximately constant (Fig. 11(b)). This is because key point 3 has a low level of stress and is almost always in an elastic stage. However, due to strong earthquake motion, it enters the plastic stage only at 7 s, resulting in irrecoverable non-elastic strain. Because the strains experienced during earthquakes are all weaker than that at 7 s, the inelastic strain at key point 3 remains almost unchanged; the inelastic strain increases substantially when concrete damage is considered, but the strain level is very low. In general, the inelastic strain of the tower body increases when damage is considered, but the trend of non-elastic strain changes remains approximately the same. This is because the dynamic response of key points 2 and 3 is determined by the structure itself as well as the load characteristics. To sum up we know considering the plasticity of concrete, the stress and strain at the key point of the intake tower can be reduced.

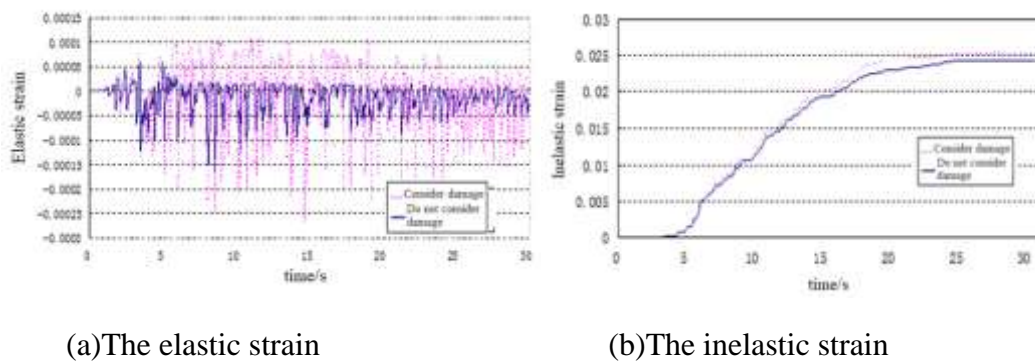


Fig. 10. The strain time-history curve of key point 2 in the tower

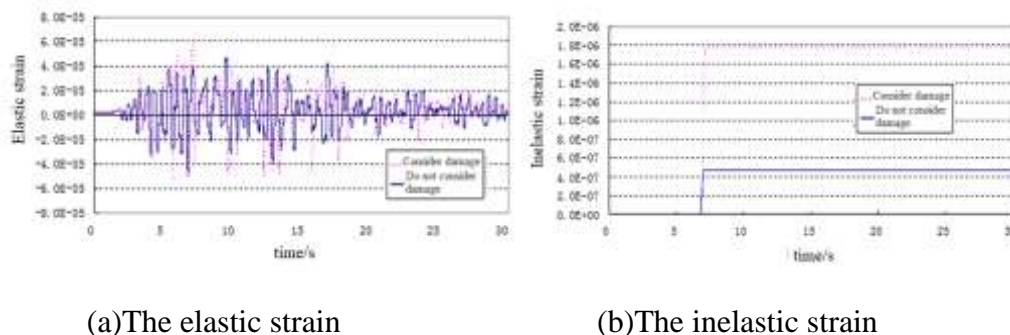


Fig. 11. The strain time-history curve of key point 3 in the tower

V. ANALYSIS OF INTAKE TOWER CRACKING

Figs. 12 and 13 illustrate that there is no concrete tension crack damage or concrete compression crack damage in the tower body at the beginning of the earthquake, indicating that the tower body is in the elastic stage under static motion, and the stress level is not high. The seismic intensity then gradually increases with time. At 5 s, minimal damage occurs in the horizontal area at the junction of the tower body and the backfill. With increasing seismic intensity, the extent of the damage increases at 10 s, and the degree of local damage is very serious. After 10 s, the earthquake intensity gradually decreases, the damaged area no longer expands, and the degree of damage is only slightly increased.

According to the tower damage cloud diagrams at the same moment, the tension damage state of the tower body is much more serious than the compression damage state (Figs. 12 and 13). This is predominantly because the concrete tensile strength is much lower than the concrete compressive strength, so the concrete is more likely to be damaged in the same location, and the tensile damage is more serious than the compressive damage; thus, damage to the tower body is predominantly caused by tensile stress. Over the entire earthquake process, the locations of tension and compression damage to the tower body are the same, i.e., at the junction of the back of the tower and the backfill concrete, as shown in Fig. 5. The development of both damage styles in this area is highly consistent in time and form, which indicates that the location and process of damage to the tower structure are determined by the tower structure itself and the characteristics of the seismic load. The occurrence of tension and compression damage is related to the earthquake process. Moreover, the simulation results of this paper are basically consistent with the experimental results of Jiang Cai [11].

According to Fig. 14, The cumulative time history curve of tension / compression damage of the intake tower further illustrates the damage development process of the intake tower, which is sudden and irrecoverable.

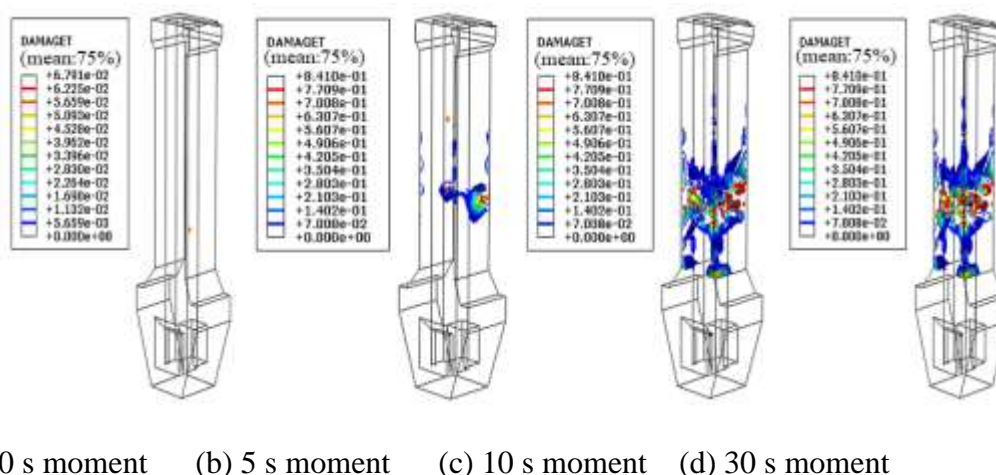
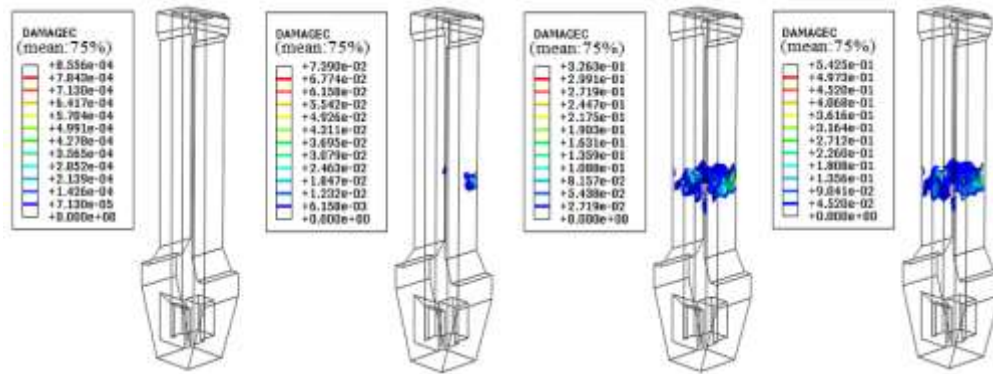
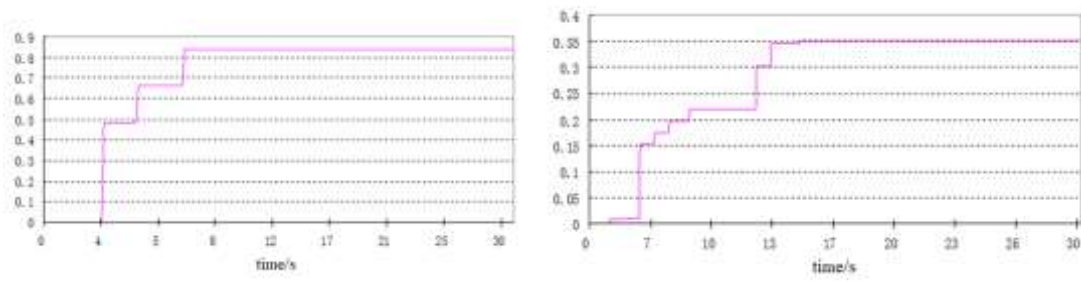


Fig. 12. Intake tower tension crack damage cloud



(a) 0 s moment (b) 5 s moment (c) 10 s moment (d) 30 s moment

Fig. 13. Intake tower compression crack damage cloud



(a) The tension damage (b) The compression damage

Fig. 14. The accumulative time-history curve of damage in the intake tower

VI. CONCLUSION

This study employs the concrete elastic-plastic damage constitutive model and data from an actual intake tower engineering project to establish a 3D finite element model of the tower body and foundations using ABAQUS software. The seismic response of the intake tower is analyzed in both the situation of considering and neglecting concrete damage. The conclusions of the study are as follows:

(1) The stress in the intake tower with concrete damage is greater than that without the damage. However, the inelastic strains are approximately the same. This is because the dynamic response of the intake tower is determined by the structure itself and the load characteristics.

(2) The junction between the tower body and the backfill concrete is the weak part of the structure where the tower body is damaged and cracked during earthquake motion. With earthquake duration increases, the extent and degree of damage to the intake tower increases; the damaged area expand to all sides. The main expansion direction is horizontal.

(3) After considering the damage of concrete, the displacement of the tower increases, the stress and strain increase, and the damage scope increases, so the nonlinear analysis results considering the damage of concrete are less safe, but it is more in line with the actual engineering.

(4) Because of the fluid-solid coupling theory research was still less in the intake tower structure, this paper uses the Westergaard additional mass method to analyze the water body, and does not consider the influence of the real water body on the intake tower. Therefore, it is necessary to further study the influence of the fluid structure interaction of the intake tower.

ACKNOWLEDGEMENTS

This research was supported by the Open Fund Project of State Key Laboratory of Eco-hydraulics in Northwest Arid Region (Grant No.2019KFKT-15), the Project of Water Resources Scientific Research and extension in Hebei Province (Grant No. 2020-11), Innovation funding project for graduate students in Hebei Province (Grant No. CXZZBS2019166), Natural Science Foundation of Hebei Province (E2020402087), Science and Technology Research Program of Chongqing Education Commission (KJQN202103602), Handan Science and Technology Bureau projects (21422051264).

REFERENCES

- [1] Chen H.Q., Guo S.S. (2012) Seismic damage analysis of high concrete dam-foundation system. *Journal of Hydraulic Engineering*, Vol.43, No.1, P: 2-7.
- [2] Ma H.F., Chen H.Q., Xu S.F. (2012) Review on the advance of seismic response analysis of high concrete dam systems under strong earthquake. *Journal of China Institute of Water Resources and Hydropower Research*, Vol.10, No.1, P: 1-8.
- [3] Chen H.Q. (2017) Challenge Confronted in Seismic Design of High Concrete Dams. *Hydropower and Pumped Storage*, Vol.3, No.2, P: 1-13.
- [4] Zheng X.D., Liu Y.H., Zhang W.J., Cao W. (2016) A Tensile Plastic Damage Constitutive Model of Concrete Based on Energy. *International Journal of Earth Sciences and Engineering*, Vol.09, No.05, P: 2241-2248.
- [5] Li N., Li Q., Ren T., Lei G.Y. (2014) Dynamic Response Analysis of Zipingpu Intake Tower under Wenchuan Earthquake Action. *Chinese Journal of Underground Space and Engineering*, Vol.10, No.5, P: 1127-1134.
- [6] Zhao J., Yang J., Li X. N. (2021). Seismic performance of intake tower structures based on endurance time method. *China Earthquake Engineering Journal*, Vol. 43, No.5, P: 1244-1250.
- [7] Gong C. L., Liu H., Zhang J. (2014). Study on Dynamic Properties of the Intake Tower with Finite Element Method. *Applied Mechanics & Materials*, Vol.501, P: 1888-1891.
- [8] Lin G., Liu J., Hu Z. Q. (2010) Current situation and progress of research on damage constitutive relation of concrete. *JOURNAL OF DALIAN UNIVERSITY OF TECHNOLOGY*, Vol.50, No.6, P: 1055-1064.
- [9] Liu Y.Q., Zhao L.H., Qian W. J. (2015) Simulation analysis on seismic damage of intake tower of Shapai Hydropower Station. *Water Resources and Hydropower Engineering*, Vol.46, No.1, P: 30-33.
- [10] Hu Y.H., Bao T.F., Zhu Z., Gong J. (2021) Influence of Pile Foundation on Dynamic Stability of Intake Tower Foundation. *China Earthquake Engineering Journal*, Vol.43, No.3, P: 728-736.
- [11] Jiang C., Zhang L.J., Zhang H.Y., etc. (2021) Non-contact measurement technique-based experimental study on dynamic failure model for intake tower. *Water Resources and Hydropower Engineering*, Vol.52, No.1, P: 64-70.

- [12] Zheng X.D. (2017). Analysis of the Earthquake Damage Mechanism of High Intake Tower, Xi'an: Xi'an University of Technology.
- [13] Kabutey A., Herák D., Dajbych O. et al. (2014). Deformation energy of *Jatropha curcas* L. seeds under compression loading. *Research in Agricultural Engineering*, Vol.60, P: 68-74.
- [14] Ren X.D., Zeng S.J., Li J. (2015) A rate-dependent stochastic damage-plasticity model for quasi-brittle materials. *Computational Mechanics*. Vol.55, No.2, P: 267-285. DOI: 10.1007/s00466-014-1100-7
- [15] Ministry of Water Resources of the People's Republic of China (2016). Specification for load design of hydraulic structures (SL 744-2016), Beijing: China Water & Power Press.
- [16] Ministry of Water Resources of the People's Republic of China (2018). Design code for hydraulic concrete structures (SL 191-2018), Beijing: China Water & Power Press.
- [17] Altunisik, A. C., & Sesli, H. (2015). Dynamic response of concrete gravity dams using different water modelling approaches: westergaard, lagrange and euler. *Computers and Concrete*, Vol.16, No.3, P: 429-448.
- [18] Dang K.N., Liu Y.H., Wang Y., Kong L., Yue X. (2017) Study and discussion on hydrodynamic pressure at intake tower of hydropower station. *Water Resources and Hydropower Engineering*, Vol.48, No.4, P: 72-78.